

AD-A049 118

NAVAL RESEARCH LAB WASHINGTON D C
RUNAWAY ELECTRONS IN COLLECTIVE ELECTRIC FIELDS, (U)
SEP 77 B H HUI, N K WINSOR

F/G 20/9

UNCLASSIFIED

NRL-MR-3614

SBIE-AD-E000 047

E(49-20)-1006

NL

| OF |
AD
A049118



END
DATE
FILMED
3 - 78
DDC

AD A049118

adl 000047

AD No. _____
DDC FILE COPY

12
13.5

NRL Memorandum Report 3614

Runaway Electrons In Collective Electric Fields

BERTRAM H. HUI

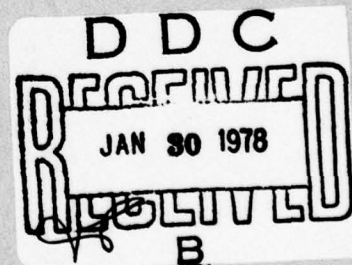
*Science Applications, Inc.
McLean, Virginia 22101*

and

N. WINSOR

*Plasma Dynamics Branch
Plasma Physics Division*

September 1977



NAVAL RESEARCH LABORATORY
Washington, D.C.

SECURITY CLASSIFICATION OF THIS PAGE (When Data Entered)

REPORT DOCUMENTATION PAGE		READ INSTRUCTIONS BEFORE COMPLETING FORM
1. REPORT NUMBER NRL-MK-3614	2. GOVT ACCESSION NO.	3. RECIPIENT'S CATALOG NUMBER 9
4. TITLE (and Subtitle) RUNAWAY ELECTRONS IN COLLECTIVE ELECTRIC FIELDS	5. TYPE OF REPORT & PERIOD COVERED Interim report on a continuing NRL problem	
6. AUTHOR(s) Bertram H. Hui and Niels K. Winsor	6. PERFORMING ORG. REPORT NUMBER	
7. PERFORMING ORGANIZATION NAME AND ADDRESS Naval Research Laboratory Washington, D. C. 20375	8. CONTRACT OR GRANT NUMBER(s)	
9. CONTROLLING OFFICE NAME AND ADDRESS U.S. Energy Research and Development Administration Washington, D. C. 20545	10. PROGRAM ELEMENT, PROJECT, TASK AREA & WORK UNIT NUMBERS NRL Problem H02-37 E(49-20)-1006	
11. MONITORING AGENCY NAME & ADDRESS (if different from Controlling Office) SBIE	12. REPORT DATE Sep 1977	
13. DISTRIBUTION STATEMENT (of this Report) Approved for public release; distribution unlimited. AD-E000-0477	13. NUMBER OF PAGES 18	
14. DISTRIBUTION STATEMENT (of the abstract entered in Block 20, if different from Report)	15. SECURITY CLASS. (of this report) UNCLASSIFIED	
15. SUPPLEMENTARY NOTES This research was sponsored by the U.S. Energy Research and Development Administration under Subtask E(49-20)-1006. *Science Applications, Inc.	15a. DECLASSIFICATION/DOWNGRADING SCHEDULE	
16. KEY WORDS (Continue on reverse side if necessary and identify by block number) Anomalous resistivity Tokamaks Computer simulation	17. ABSTRACT (Continue on reverse side if necessary and identify by block number) The interactions of runaway electrons with the anomalous-Doppler shifted mode and a bump-on-tail mode are studied numerically using the Fokker-Planck equation with a self-consistent quasilinear diffusion operator. The resulting frequency spectrum and the synchrotron radiation power agree with the experimental observations. Furthermore, we show that there is a velocity threshold, below which electrons are not pitch-angle scattered by the self-consistent electric fields. The observed long-time behavior of synchrotron radiation data implies that this velocity threshold must shift to higher velocity as an experiment progresses.	

DDC
RECEIVED
JAN 30 1978
B

251950

YB

SECURITY CLASSIFICATION OF THIS PAGE (When Data Entered)

REPORT DOCUMENTATION PAGE	
1. REPORT NUMBER	
2. AUTHOR	
3. TITLE	
4. INSTITUTION	
5. PERFORMING ORGANIZATION	
6. AUTHORING ORGANIZATION	
7. PERFORMING ORGANIZATION	
8. PERFORMING ORGANIZATION	
9. PERFORMING ORGANIZATION	
10. PERFORMING ORGANIZATION	
11. PERFORMING ORGANIZATION	
12. PERFORMING ORGANIZATION	
13. PERFORMING ORGANIZATION	
14. PERFORMING ORGANIZATION	
15. PERFORMING ORGANIZATION	
16. PERFORMING ORGANIZATION	
17. PERFORMING ORGANIZATION	
18. PERFORMING ORGANIZATION	
19. PERFORMING ORGANIZATION	
20. PERFORMING ORGANIZATION	
21. PERFORMING ORGANIZATION	
22. PERFORMING ORGANIZATION	
23. PERFORMING ORGANIZATION	
24. PERFORMING ORGANIZATION	
25. PERFORMING ORGANIZATION	
26. PERFORMING ORGANIZATION	
27. PERFORMING ORGANIZATION	
28. PERFORMING ORGANIZATION	
29. PERFORMING ORGANIZATION	
30. PERFORMING ORGANIZATION	
31. PERFORMING ORGANIZATION	
32. PERFORMING ORGANIZATION	
33. PERFORMING ORGANIZATION	
34. PERFORMING ORGANIZATION	
35. PERFORMING ORGANIZATION	
36. PERFORMING ORGANIZATION	
37. PERFORMING ORGANIZATION	
38. PERFORMING ORGANIZATION	
39. PERFORMING ORGANIZATION	
40. PERFORMING ORGANIZATION	
41. PERFORMING ORGANIZATION	
42. PERFORMING ORGANIZATION	
43. PERFORMING ORGANIZATION	
44. PERFORMING ORGANIZATION	
45. PERFORMING ORGANIZATION	
46. PERFORMING ORGANIZATION	
47. PERFORMING ORGANIZATION	
48. PERFORMING ORGANIZATION	
49. PERFORMING ORGANIZATION	
50. PERFORMING ORGANIZATION	
51. PERFORMING ORGANIZATION	
52. PERFORMING ORGANIZATION	
53. PERFORMING ORGANIZATION	
54. PERFORMING ORGANIZATION	
55. PERFORMING ORGANIZATION	
56. PERFORMING ORGANIZATION	
57. PERFORMING ORGANIZATION	
58. PERFORMING ORGANIZATION	
59. PERFORMING ORGANIZATION	
60. PERFORMING ORGANIZATION	
61. PERFORMING ORGANIZATION	
62. PERFORMING ORGANIZATION	
63. PERFORMING ORGANIZATION	
64. PERFORMING ORGANIZATION	
65. PERFORMING ORGANIZATION	
66. PERFORMING ORGANIZATION	
67. PERFORMING ORGANIZATION	
68. PERFORMING ORGANIZATION	
69. PERFORMING ORGANIZATION	
70. PERFORMING ORGANIZATION	
71. PERFORMING ORGANIZATION	
72. PERFORMING ORGANIZATION	
73. PERFORMING ORGANIZATION	
74. PERFORMING ORGANIZATION	
75. PERFORMING ORGANIZATION	
76. PERFORMING ORGANIZATION	
77. PERFORMING ORGANIZATION	
78. PERFORMING ORGANIZATION	
79. PERFORMING ORGANIZATION	
80. PERFORMING ORGANIZATION	
81. PERFORMING ORGANIZATION	
82. PERFORMING ORGANIZATION	
83. PERFORMING ORGANIZATION	
84. PERFORMING ORGANIZATION	
85. PERFORMING ORGANIZATION	
86. PERFORMING ORGANIZATION	
87. PERFORMING ORGANIZATION	
88. PERFORMING ORGANIZATION	
89. PERFORMING ORGANIZATION	
90. PERFORMING ORGANIZATION	
91. PERFORMING ORGANIZATION	
92. PERFORMING ORGANIZATION	
93. PERFORMING ORGANIZATION	
94. PERFORMING ORGANIZATION	
95. PERFORMING ORGANIZATION	
96. PERFORMING ORGANIZATION	
97. PERFORMING ORGANIZATION	
98. PERFORMING ORGANIZATION	
99. PERFORMING ORGANIZATION	
100. PERFORMING ORGANIZATION	

RECEIVED
JAN 20 1978
B D C

SECURITY CLASSIFICATION OF THIS PAGE(When Data Entered)

CONTENTS

I. INTRODUCTION	1
II. ANALYTICAL MODEL	2
III. NUMERICAL MODEL	5
IV. NUMERICAL RESULTS	6
V. SUMMARY	8

ACCESSION for		
NTIS	Wide Section	<input checked="" type="checkbox"/>
DDC	Brief Section	<input type="checkbox"/>
UNANNOUNCED		<input type="checkbox"/>
JUSTIFICATION		
BY		
DISTRIBUTION/AVAILABILITY CODES		
Dist.	AVAIL. and/or	SPECIAL
A		

RUNAWAY ELECTRONS IN COLLECTIVE ELECTRIC FIELDS

I INTRODUCTION

Recently, there have been numerous reports¹⁻⁶ of runaway electrons in tokamaks. The energy of runaway electrons observed in low density discharges ($n \leq 10^{13} \text{ cm}^{-3}$) is lower than that observed in higher density discharges. It has also been observed that the synchrotron radiation power often increases in steps, and is accompanied by radiation near and below the plasma frequency (ω_{pe}). As first pointed out by Coppi et. al.,⁷ the reduced plasma frequency radiation ($\omega_k = k_{||} / k \omega_{pe}$) in Alcator could be explained by an anomalous Doppler shifted mode,⁸ where ω_k is the wave frequency, k is the wave number, and $k_{||}$ is its component in the toroidal magnetic field direction. Pitch-angle scattering of the runaway electrons by the anomalous-Doppler-shifted mode can lead to an increase of synchrotron radiation.^{5,9} Papadopoulos et al.¹⁰ also show that pitch-angle scattering can cause a bump to form on the tail of the electron distribution. The bump-on-tail instability will then be excited and give rise to the ω_{pe} mode which is observed. Moreover, anomalous-Doppler-shifted and bump-on-tail modes may cause many runaway electrons to become trapped in local mirrors,¹¹ ∇B drift to the wall of the vacuum vessel, and destroy its liner. Such liner destruction may have been observed by the TFR group.² The macroscopic behavior of the anomalous-Doppler-shifted mode is described in detail by Choi and Horton.¹²

In this paper, we study the interactions between the runaway electrons and the collective modes using a Fokker-Planck model including a self-consistent quasilinear diffusion term. First, we show that if only the anomalous-Doppler-shifted mode is present, it gives rise to the bump-on-tail distribution. This is because of a velocity threshold for the anomalous-Doppler-shifted mode. Second, we show that the combination of the anomalous-Doppler-shifted mode, the bump-on-tail mode and a weak toroidal electric field $E_{||}$, can lead to synchrotron radiation similar to that experimentally observed. In section II, we review the analytical theory. In section III, we present the numerical model. The results are given in section IV, and these results are summarized in section V.

Note: Manuscript submitted September 14, 1977.

II ANALYTICAL MODEL

For electrostatic waves in a homogeneous magnetic field with immobile ions, we use the Harris dispersion relation:

$$k^2 = \omega_{pe}^2 \int dv \sum_l \frac{J_l^2(k_\perp v_\perp / \omega_{ce})}{k_\parallel v_\parallel - \omega_k - l\omega_{ce}} \times \left[k_\parallel v_\parallel \frac{\partial f_{oe}}{\partial v_\parallel^2} - l\omega_{ce} \frac{\partial f_{oe}}{\partial v_\perp^2} \right], \quad (1)$$

where J_l is the Bessel function of the first kind of order l , and ω_{ce} is the electron cyclotron frequency.

The initial distribution f_{oe} is given by a sum of a bulk equilibrium and a "tail" Maxwellian; i.e.,

$$f_{oe} = f_o + f_T,$$

where

$$f_o = n_o \left(\frac{m_e}{2\pi T_e} \right)^{3/2} \exp \left(-\frac{m_e v^2}{2T_e} \right),$$

and

$$f_T = n_T \left(\frac{m_e}{2\pi} \right)^{3/2} \frac{1}{T_{\perp T} T_{\parallel T}^{1/2}} \exp \left(-\frac{m_e v_\perp^2}{2T_{\perp T}} - \frac{m_e v_\parallel^2}{2T_{\parallel T}} \right),$$

with $n_T \ll n_o$ and $T_{\parallel T} \gg T_{\perp T}$ and $T_e \approx T_{\perp T}$. We expect that the dominant contributions to the growth rate γ_k^A come from $l = 0, -1$ gyroresonances because the $l = +1$ resonance is at the negative velocity side where the distribution function is relatively small. Solving the dispersion relation with $k_\perp v_\perp / \omega_{ce} \ll 1$ and keeping only the $l = 0$ and -1 terms, we obtain:

$$\omega_k \approx k_\parallel / k \omega_{pe} \quad (2)$$

and,

$$\begin{aligned}
\gamma_k^A \approx & \frac{\pi}{2} \frac{\omega_{pe}^3 k_{||}}{k^3} \frac{\partial \hat{f}_0}{\partial v_{||}} \bigg|_{v_{||} = \omega_k/k_{||}} \\
& + \frac{\pi}{4} \frac{k_{||}^3}{k^3} \frac{\omega_{pe}^3 v_{th\perp}^2}{\omega_{ce}^2} \frac{\partial \hat{f}_T}{\partial v_{||}} \bigg|_{v_{||} = (\omega_k + \omega_{ce})/k_{||}} \\
& + \frac{\pi}{4} \frac{k_{\perp}^2}{k^3} \frac{\omega_{pe}^3}{\omega_{ce}} \hat{f}_T \bigg|_{v_{||} = (\omega_k + \omega_{ce})/k_{||}}, \quad (3)
\end{aligned}$$

where $v_{th\perp} = (2T_e/m_e)^{1/2}$ is the perpendicular velocity of the bulk and also the tail of the distribution function, and $\hat{f} \equiv 2\pi \int_0^\infty dv_{\perp} v_{\perp} f$. The first and second term of (3) correspond to Landau damping by the $\ell = 0$ and $\ell = -1$ terms respectively. The third term is the driving term for the instability and is directly proportional to the density of the tail. The most unstable anomalous-Doppler-shifted mode¹³ has $k_{\perp} = \sqrt{2}k_{||}$.

Let us examine the circumstances under which these modes become important. We can estimate the resonance width in velocity space of the $\ell = 0$ and $\ell = -1$ resonances, given the maximum tail velocity v_m . In order for $\gamma_k^A > 0$, the third term of (3) has to be, bigger than the first term, i.e. Landau damping (the second term usually is not as important). To avoid Landau damping, we usually need $\omega_k/k_{||} > 3v_{th}$. But at resonance, $v_m = (\omega_{ce} + \omega_k)/k_{||}$, so $\omega_k/k_{||} \leq \omega_k v_m / (\omega_{ce} + \omega_k)$. Thus for the $\ell = 0$ resonance, $3v_{th} < v_{||} \leq \omega_k v_m / (\omega_{ce} + \omega_k)$, and for the $\ell = -1$ resonance, we have $3v_{th}(\omega_{ce} + \omega_k)/\omega_k < v_{||} \leq v_m$. In ATC, for example with $\omega_{ce} = \omega_{pe}$ and for runaway electron energy with $v_m = 10v_{th}$ and $k_{\perp} = \sqrt{2}k_{||}$ (which corresponds to maximum growth), we find for $\ell = 0$: $3v_{th} < v_{||} \leq 3.7v_{th}$, and for $\ell = -1$ we find: $8v_{th} < v_{||} \leq 10v_{th}$. For $T_e \approx 1\text{KeV}$, this will correspond to a runaway tail of about 140 KeV.

Once the anomalous-Doppler-shifted instability is excited, the self-consistent fluctuating electric fields will pitch-angle scatter the tail electrons. This process tends to isotropize the tail of the runaway electron distribution. Since a threshold exists for the $\ell = -1$ resonance, there is no pitch-angle scattering outside the resonant region of $v_{||}$. As the high-parallel-energy particles are continuously be-

ing isotropized, this causes an increase of electron density near the threshold of the $\ell = -1$ resonance. As was first pointed out by Papadopoulos¹⁰, this process modifies the runaway distribution function, forming a bump-on-tail distribution. This result is confirmed by both particle simulations and numerical Fokker-Planck solutions¹⁴.

The growth rate γ_k^B and ω_k^B for the two-dimensional bump-on-tail case are¹⁵:

$$\omega_k^B = \frac{1}{1 + \alpha^2} \left\{ \omega_{pi}^2 + \left(\frac{k_{||}}{k} \right)^2 \omega_{pe}^2 \right\}, \quad (4)$$

and

$$\gamma_k^B = -\omega_k^B \left[\pi^{1/2} \frac{n_T}{n_0} \frac{\omega_{pe}^2}{k^2 v_{th\perp}^2 (1 + \alpha^2)} \zeta \exp(-\zeta^2) \right], \quad (5)$$

where

$$\zeta = (\omega_k^B - k_{||} v_b) / k_{||} v_{th\perp},$$

and

$$\alpha^2 = \frac{\omega_{pe}^2}{\omega_{ce}^2} - \frac{n_T}{n_0} \frac{\omega_{pe}^2}{k^2 v_{th\perp}^2} \text{Re}Z'(\zeta),$$

where ω_{pi} is the ion plasma frequency, v_b is the velocity of the bump, and $\text{Re}Z'(\zeta)$ is the real part of the derivative of the Plasma Dispersion function. Depending on the angle of propagation, ω_k^B covers a range from ω_{pi} to ω_{pe} .

III NUMERICAL MODEL

The time evolution of the distribution function, anomalous-Doppler-shifted modes, and bump-on-tail modes is determined by the Fokker-Planck equation with a quasilinear diffusion operator:

$$\frac{\partial f_{oe}}{\partial t} - \frac{e}{m} \mathbf{E} \cdot \frac{\partial f_{oe}}{\partial \mathbf{v}} = \left(\frac{\partial f_{oe}}{\partial t} \right)_c + \nabla \cdot \mathbf{D} \cdot \nabla f_{oe} \quad (6)$$

where

$$\frac{1}{\Gamma_e} \left(\frac{\partial f_{oe}}{\partial t} \right)_c = -\nabla \cdot (f_e \nabla h_e) + \frac{1}{2} \nabla \nabla : (f_e \nabla \nabla g_e). \quad (7)$$

Here h_e and g_e are the "Rosenbluth potentials",

$$g_e(\mathbf{v}) = \sum_{b=e,i} \int d\mathbf{v}' f_{ob}(\mathbf{v}') |\mathbf{v} - \mathbf{v}'|,$$

$$h_e(\mathbf{v}) = \sum_{b=e,i} \frac{m_e + m_b}{2 m_b} \nabla^2 g_e,$$

with

$$\Gamma_e = (4\pi e^4 \ln D_e) / m_e^2,$$

and

$$D_e = \frac{3T_e}{2e^2} \left(\frac{T_e}{\pi n_e e^2} \right)^{1/2}.$$

The diffusion operation in Eq. (6) is given by¹⁷

$$\begin{aligned} \nabla \cdot \mathbf{D} \cdot \nabla f_{oe} = & 8\pi \frac{e^2}{m^2} \sum_{\mathbf{k}} \int d\mathbf{k} \frac{\mathcal{E}_{\mathbf{k}}(t)}{k^2} \left[\frac{-\mathbf{k} \omega_{ce}}{v_{\perp}} \frac{\partial}{\partial v_{\perp}} \right. \\ & \left. + k_{\parallel} \frac{\partial}{\partial v_{\parallel}} \right] \frac{J_{\perp}^2(k_{\perp} v_{\perp} / \omega_{ce})}{-i\omega_{\mathbf{k}} + ik_{\parallel} v_{\parallel} - i\mathbf{k} \omega_{ce} + \gamma_{\mathbf{k}}} \left[\frac{-\mathbf{k} \omega_{ce}}{v_{\perp}} \frac{\partial}{\partial v_{\perp}} \right. \end{aligned}$$

$$\left(+ k_{\parallel} \frac{\partial}{\partial v_{\parallel}} \right) f_{oe}, \quad (8)$$

where

$$\frac{\partial \mathcal{E}_k(t)}{\partial t} = 2 \gamma_k \mathcal{E}_k(t) + \text{thermal fluctuations} \quad (9)$$

and γ_k is given by (3) and (5).

Eq. (2)-(9) are solved numerically in polar coordinates using an alternating-direction-implicit method.^{18,19} Since it is impractical to cover all directions of the wave vector \mathbf{k} , we choose to solve the case where γ_k is maximum, i.e., $k_{\perp} = \sqrt{2} k_{\parallel}$. We hasten to point out that this does not mean we are restricting to one mode, because for this chosen propagation angle, the magnitude of k still varies.

IV NUMERICAL RESULTS

In previous work^{10,14} we examined the consequences of the bum-on-tail structure. Considerable interest has since been shown in the actual formation of this bump-on-tail distribution. We therefore present here two types of numerical experiments; one which shows how the bump-on-tail distribution forms, and one which shows the complete dynamics of the electron distribution.

We shall perform these calculations for Adiabatic Toroidal Compressor (ATC) experimental parameters. Our theory predicts that the electrons of interest are only mildly relativistic, so neither theory nor computation need be concerned with relativistic corrections. The Alcator experiment, in contrast, has $\omega_{ce} \gg \omega_{pe}$, and the bump-on-tail electrons are expected to be highly relativistic.

We begin by artificially removing the bump-on-tail process from the physical model, to show how the ADS modes can produce the bump on the tail of the distribution function. We

model the ATC experimental conditions as follows: $\omega_{ce} = \omega_{pe}$, $n_e = n_i = 2 \times 10^{13} \text{ cm}^{-3}$, $n_T/n_e = 0.03$, $T_e = T_i = 1 \text{ kev}$, and $v_m/v_{th\perp} = 10$. Here v_m is the maximum velocity of the runaway tail, and E_r is the runaway (Dreicer) electric field.

Figure 1 shows the initial, monotonically decreasing distribution function, and the one into which it evolves in 10^{-7} sec. Note the regions of $\ell = 0$ and $\ell = -1$ resonance. The pitch-angle scattering due to these resonances produces the bump. As we will see below, the bump-on-tail modes; when present, will quickly remove a bump of this magnitude. For now, our purpose is to show that such a bump can spontaneously form from a runaway distribution, and to examine its parametric dependence.

In Fig. 2, we change $\omega_{pe}/\omega_{ce} = 1$ to $\omega_{pe}/\omega_{ce} = 1.25$ which corresponds to higher density. We see that the threshold (the bump) gets closer to the thermal region. Eventually as the density increases the bump may get so close that it may merge with the thermal region, and the bump-on-tail modes could no longer be excited.

It is the flattening of the bump, and the resulting bump-on-tail modes, which accounts for the slowing down of the runaway electrons. Therefore, we expect that, in high density operations where the bump approaches the thermal distribution the runaway electron energy is higher, since the bump-on-tail modes provide less energy loss.

When we switch on the bump-on-tail mode, we do not expect to see the bump anymore, because the bump-on-tail mode occurs on a much faster time scale and flattens any bump. In Fig. 2, we show the time development of $\hat{f}(v_{||})$ with both the anomalous-Doppler-shifted and bump-on-tail modes present. The parameters are the same as Fig. 1 except $n_T/n_o = 2\%$. The dotted curve shows the distribution function at steady state, about $1 \mu\text{sec.}$ after initiation.

Note that no bump is formed, and $\hat{f}(v_{||})$ is flatter at the tail than initially. We find the

anomalous-Doppler-shifted instability dies down because of the depletion of particles by the $\ell = -1$ resonance. This is consistent with (3) which says the growth rate is directly proportional to the magnitude of \hat{f} at the $\ell = -1$ resonance.

We have also calculated the synchrotron radiation power due to uncorrelated electrons and find that the power increases by about 75% in about 1 μ sec (See Fig. 4) and levels off after the instabilities die down. This is consistent with experimental observations.⁵ We conclude that the excitation of the anomalous-Doppler-shifted mode is definitely related to the increase of synchrotron radiation. If we follow $\hat{f}(v_{||})$ longer, we expect the resonance region of $\ell = -1$ to be filled up again, because $E_{||}$ can accelerate particles from low $v_{||}$ to high $v_{||}$. When this happens, the instability should be excited again and the synchrotron radiation should also increase. We have followed $\hat{f}(v_{||})$ up to 2.8×10^{-4} sec when the tail region is almost filled up again (see the circles of Fig. 2). We find the instability is not excited because the negative slope at $\ell = 0$ also increases tremendously. At first we believed this was due to $E_{||}$ pushing the bulk electrons, but we found this effect still remained after we switched off $E_{||}$. We conclude this must be due to isotropization. In fact it can be easily estimated that complete isotropization of $\hat{f}(v_{||})$ at $v_{||} = 3 v_{th}$ takes about 1 msec. Therefore in about a third of this time, the slope can increase enough to damp out the anomalous-Doppler-shifted mode. Experimentally it is observed that the synchrotron radiation increases in steps a few msec apart. If the increase in radiation is related to the excitation of anomalous-Doppler-shifted mode which we think it is, then v_m and the instability threshold for anomalous-Doppler-shifted mode must increase so that the $\ell = 0$ resonant region can reach $4 v_{th}$ or $5 v_{th}$.

V SUMMARY

We have developed the analytic tools for describing the effect of anomalous Doppler-shifted plasma waves and bump-on-tail modes upon the tokamak electron distribution func-

tion. These effects have been self-consistently incorporated in a numerical solution of the Fokker-Planck equation as a quasi-linear diffusion operator. Based on results using this model, we find the following general properties of the tokamak electron distribution:

1. The onset of the anomalous-Doppler-shifted modes gives rise both to a suprathermal synchrotron radiation spectrum and formation of a bump-on-tail distribution.
2. The combination of anomalous-Doppler-shifted and bump-on-tail modes are necessary to slow down the runaway electrons.

When comparing different experiments, our studies predict:

3. Experiments at higher electron number density should show lower-amplitude anomalous-Doppler-shifted modes, and higher mean runaway energy.
4. At any density, the threshold in v for onset of the anomalous-Doppler-shifted mode shifts outward with time.

Finally, the sudden reduction in $v_{||}$ caused by onset of the bump-on-tail modes and resultant flattening of the electron distribution function may cause voltage spikes. This loss in $v_{||}$ takes place with minimal loss of energy, breeding very hot electrons with large v_{\perp} and small $v_{||}$. Such electrons would be trapped in poloidal magnetic field minima, and could drift to the outside of the system, leading to liner damage such as seen in TFR and Alcator.

ACKNOWLEDGMENTS

Work supported by ERDA contract no. E(49-20)-1006 We would like to thank K. Papadopoulos, C. S. Liu, Y. Mok and I. Bernstein for many helpful discussions.

REFERENCES

1. V.S. Vlasenkov, V. M. Leonov, V.G. Merezkin and V.S. Mukhovatov, Nuclear Fusion 13,

509 (1973).

2. TFR Group Vth Conf. on Plasma Physics and Controlled Fusion Research, Tokyo, Japan, Paper IAEA-CN-33/AG-2, (1974).
3. V.V. Alikae, Vu.I. Arsen'ev, G.A. Bobrovskii, A.A. Kondrat'ev and K.A. Razumova, Zh. Tekh. Fiz. **45**, 515 (1975) [Sov. Phys. Tech. Phys. **20**, 327 (1975)].
4. V.V. Alikae, K.A. Razumova and Yu.A. Sokolov, Fiz. Plazmy **1**, 546 (1975) [Sov. Physics-Plasma Physics (to be published)].
5. D.A. Boyd, F.J. Stauffer and A.W. Trivelpiece, Phys. Rev. Lett. **37**, 98 (1976).
6. H. Knoepfel, D.A. Spong, and S.J. Zweben, Phys. Fluids **20**, 511 (1977).
7. B. Coppi, F. Pegoraro, R. Pozzoli, and G. Rewoldt, Nucl. Fusion **16**, 309 (1976).
8. B.B. Kadomtsev and O.P. Pogutse, Zh. Eksp. Teor. Fiz., **53**, 2025 (1967) [Sov. Phys.-J.E.T.P. **26**, 1146 (1968)].
9. C.S. Liu and Y. Mok, Phys. Rev. Lett **38**, 162 (1977).
10. K. Papadopoulos, B. Hui, and N. Winsor, to be published in Nucl. Fusion.
11. C.S. Liu, Y. Mok and F. Englemann, International Topical Conference on Synchrotron Radiation and Runaway Electrons in Tokamaks, College Park, Maryland, U.S.A. (1977).
12. Duk-in Choi and W. Horton, Jr., FRCR No. 120, Fusion Research Center, University of Texas at Austin, Texas.
13. K. Papadopoulos, private communication
14. K. Papadopoulos, I. Haber, B. Hui, J. Huba, P. Palmadesso and N. Winsor, International Topical Conference on Synchrotron radiation and Runaway Electrons in Tokamaks, College Park, Maryland, U.S.A. (1977)
15. K. Papadopoulos and P. Palmadesso, Phys. Fluids **19**, 605 (1976).
16. M.N. Rosenbluth, W.M. MacDonald and D.L. Judd, Phys. Rev. **107**, 1 (1957).
17. R.C. Davidson, *Methods in Nonlinear Plasma Theory*, Academic Press, 1972.
18. J. Killeen and K.D. Marx, *Methods in Computational Physics*, ed. B. Alder et. al. (Academic

Press, New York, 1970) Vol. 9, p. 421.

19. R.M. Kulsrud, Y.C. Sun, N.K. Winsor, and H.A. Fallon, Phys. Rev. Lett. **31**, 690 (1973)

20. H. Dreicer, Phys. Rev. **115**, 238 (1959).

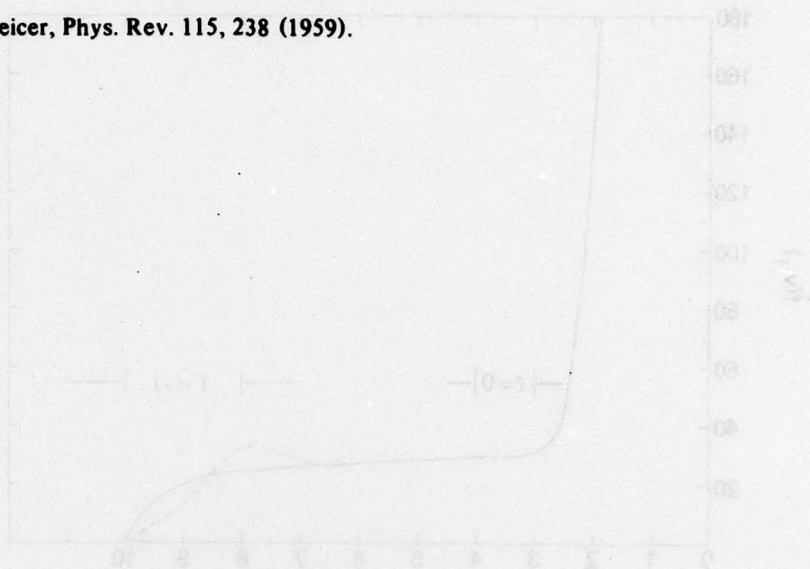


Figure 1 - Bump formation on the tail of the distribution function at $v = 10$ sec due to resonant Dreicer-strengthening with $\omega_{pe} = 1.5 \times 10^7 \text{ sec}^{-1}$, $T_e = 1 \text{ keV}$, $n = 10^{18} \text{ cm}^{-3}$, $E_0 = 0.05$ and $v_{th} = 10$. The resonance region of $v = 0$ and $v = -1$ are indicated by arrows. $f(v)$ at $v = 0$ is given by solid line.

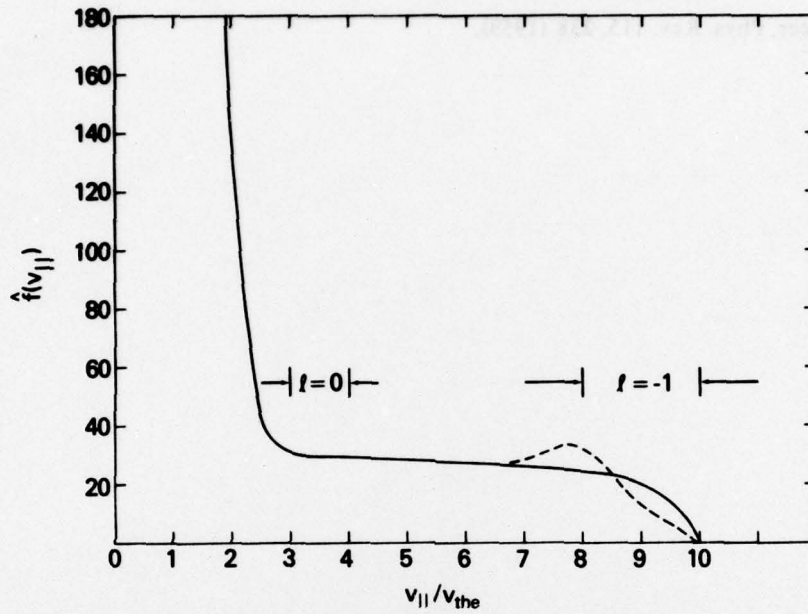


Figure 1 — Bump formation on the tail of the distribution function at $t = 10^{-7}$ sec due to anomalous-Doppler-shifted mode with $\omega_{ce}/\omega_{pe} = 1$, $n_o = 2 \times 10^{13} \text{ cm}^{-3}$, $T_e = 1 \text{ keV}$, $n_T/n_o = 3\%$, $E_{||}/E_R = 0.06$ and $v_M/v_{th\perp} = 10$. The resonance regions of $n = 0$ and $n = -1$ are indicated by arrows. $\hat{f}(v_{||})$ at $t = 0$ is given by solid line.

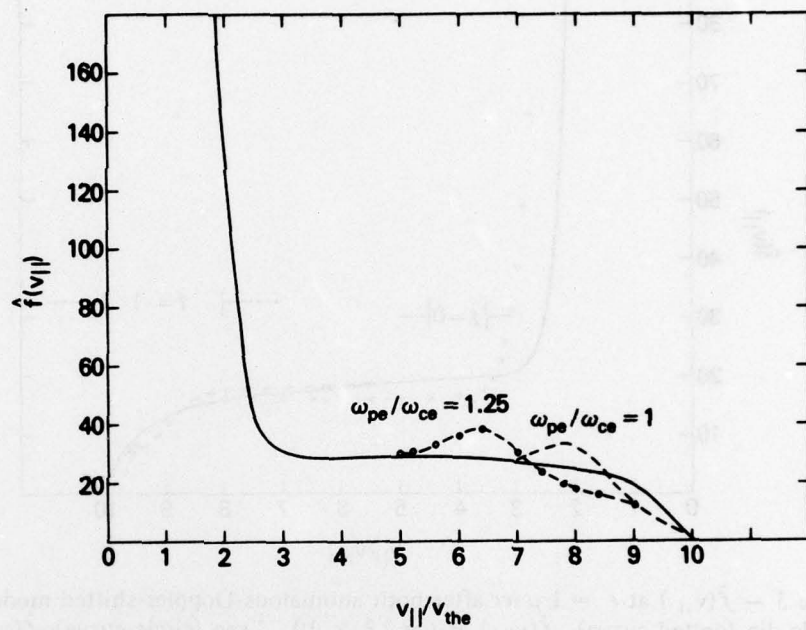


Figure 2 — Density dependence of bump formation

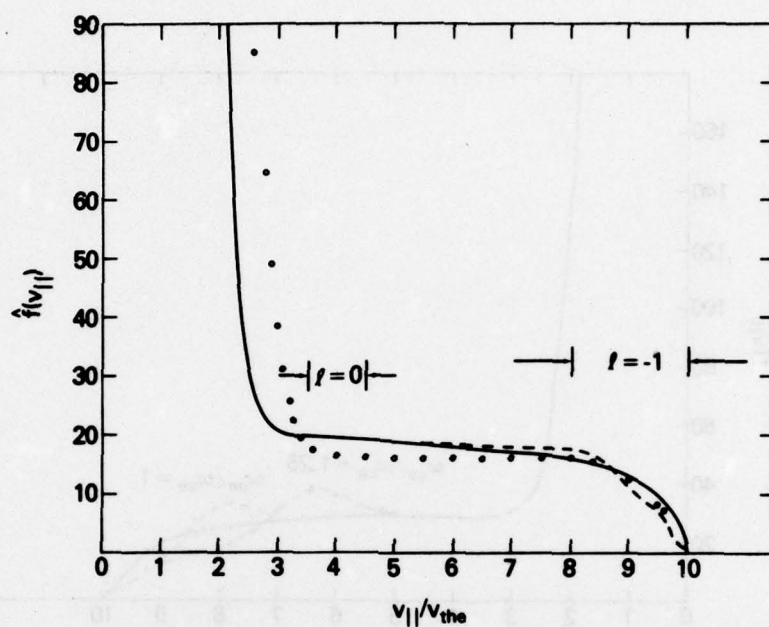


Figure 3 — $\hat{f}(v_{||})$ at $t = 1 \mu\text{sec}$ after both anomalous-Doppler-shifted mode and bump-on-tail mode die (dotted curve). $\hat{f}(v_{||})$ at $t = 2.8 \times 10^{-4} \text{ sec}$ (circle curve), $\hat{f}(v_{||})$ at $t = 0$ is given by solid line, $\omega_{ce}/\omega_{pe} = 1$, $n_o = 2 \times 10^{13} \text{ cm}^{-3}$, $T_e = 1 \text{ keV}$, $n_T/n_o = 2\%$, $E_{||}/E_R = 0.06$ and $v_M/v_{th\perp} = 10$.

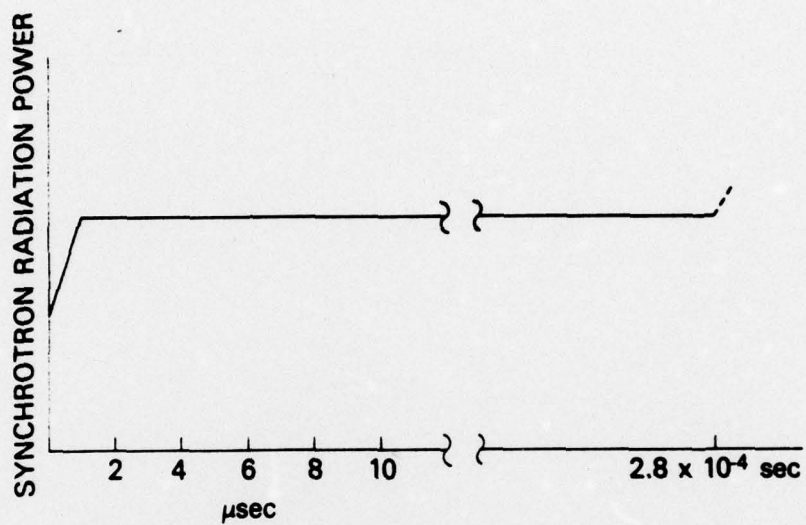


Figure 4 — Synchrotron radiation power vs time